A Nature Portfolio journal



https://doi.org/10.1038/s42003-025-08711-7

Ardipithecus ramidus ankle provides evidence for African ape-like vertical climbing in the earliest hominins

Check for updates

Thomas C. Prang **1** ⊠, Matthew W. Tocheri **2**,3,4, Biren A. Patel **5**, Scott A. Williams **6**,7 & Caley M. Orr^{8,9}

The origin of the human lineage was catalyzed by bipedalism, but how this locomotor mode evolved is debated. We investigated the evolutionary context of human bipedalism by analyzing the morphology of the 4.4 million-year-old hominin talus attributed to *Ardipithecus ramidus* (ARA-VP-6/500-023). Our results demonstrate that ARA-VP-6/500-023 bears similarities to the tali of chimpanzees and gorillas, who are adapted to vertical climbing and terrestrial plantigrade quadrupedalism. Additionally, we identify the presence of derived features in ARA-VP-6/500-023 consistent with previous suggestions of an enhanced push-off mechanism in the foot of *Ar. ramidus*. Our observations of the human and ape fossil record are inconsistent with recently proposed models of human origins, which envision the last common ancestor of humans and chimpanzees as a generalized arboreal ape. Instead, our results strongly imply that humans evolved from an African ape-like ancestor, which directly narrows the range of explanations for the origin of our lineage.

The Homo-Pan clade (i.e., extant/extinct humans, chimpanzees, and bonobos) is nested within a larger clade that includes gorillas, but major questions remain about whether the anatomy and locomotor behaviors shared among extant African apes evolved in their last common ancestor (LCA) or, alternatively, independently in Pan and Gorilla. A particularly intense debate centers on reconstructing the morphology and positional behavior of the Homo-Pan LCA, which is critical for formulating and testing hypotheses about how and why terrestrial bipedalism evolved in hominins^{1–10}. The 4.4 million-year-old partial skeleton (ARA-VP-6/500) of Ardipithecus ramidus provides especially important comparative evidence for this debate due to its hominin craniodental synapomorphies, which provide evidence for a close phylogenetic relationship between Ar. ramidus and later hominins. ARA-VP-6/500 predates postcranial fossils of Australopithecus anamensis and Australopithecus afarensis, including the 'Lucy' skeleton (A.L. 288-1), and combines primitive features, such as a grasping hallux, with derived features of the cranial base, pelvis, and foot, suggesting that Ar. ramidus used an early form of bipedalism¹⁻⁵. Therefore, the earlier adaptive grade represented

by $Ar.\ ramidus$ may shed light on the locomotor antecedents of hominin bipedalism.

The extent to which the Ar. ramidus fossils display African ape-like affinities, and their implications for locomotor behavior in the Homo-Pan LCA, is important for testing earlier models for human origins (reviewed by ref. 10), but it is currently debated. Some studies have suggested that Ar. ramidus lacks extant African ape-like adaptations to vertical climbing, terrestrial quadrupedalism (knuckle walking in particular), and below-branch suspension^{2,5}. If correct, this implies that the locomotor repertoire of the Homo-Pan LCA probably excluded these behaviors, and extensive homoplasy occurred in the evolution of hominins and African apes. After conducting a broad comparative analysis of postcranial morphology, Lovejoy and colleagues² concluded, "Ar. ramidus implies that African apes are adaptive cul-de-sacs rather than stages in human emergence" (p. 104). However, later studies suggested that Ar. ramidus possessed an African apelike foot morphology reflecting a heel-strike plantigrade foot posture⁶ combined with features enabling more effective lateral push-off in an early form of bipedalism^{1,7,8}. Moreover, the Ar. ramidus hand displays relatively

¹Department of Anthropology, Washington University in St. Louis, St. Louis, MO, USA. ²Department of Anthropology, Lakehead University, Thunder Bay, Canada. ³Human Origins Program, Department of Anthropology, National Museum of Natural History, Smithsonian Institution, Washington, DC, USA. ⁴Australian Research Council Centre of Excellence for Australian Biodiversity and Heritage, University of Wollongong, Wollongong, Australia. ⁵Division of Integrative Anatomical Sciences, Department of Medical Education, Keck School of Medicine, University of Southern California, Los Angeles, CA, USA. ⁶Center for the Study of Human Origins, Department of Anthropology, New York University, New York, NY, USA. ⁷New York Consortium in Evolutionary Primatology, New York, NY, USA. ⁸Department of Cell and Developmental Biology, University of Colorado School of Medicine, Aurora, CO, USA. ⁹Department of Anthropology, University of Colorado Denver, Denver, CO, USA. □e-mail: prang@wustl.edu

long, curved manual proximal phalanges, deep metacarpophalangeal and interphalangeal joints, and an overall shape more closely aligned with chimpanzees and bonobos than any other primate. Collectively, these features of *Ar. ramidus* suggest that climbing and below-branch suspension were components of its varied positional repertoire⁹.

Although below-branch suspension has many established morphological correlates (e.g., increased mobility at the shoulder, elbow, and wrist joints), the relationship between hind limb anatomy and vertical climbing is not as well understood. Vertical climbing is defined as the vertical ascent (and subsequent descent) of supports oriented at 45° or greater relative to the ground¹¹. All primates climb proficiently, including orangutans^{12,13} and hylobatids¹⁴, but vertical climbing constitutes a high proportion of the arboreal locomotor repertoire of African apes and represents a key element of their ecological adaptation as large-bodied, forest-living quadrupeds that utilize both arboreal and terrestrial substrates 10,11,15-22. Locomotor data compiled by Gebo²¹ shows that the arboreal locomotion of Pan troglodytes^{15–17,19,20}, Pan paniscus²⁰, and Gorilla gorilla²³ includes the highest proportion of vertical climbing (49-56%, 41%, and 56%, respectively) among the anthropoids sampled, followed by Papio anubis¹⁶ (21%) and Ateles geoffroyi²⁴ (16%). Baboons use a 'pulse' vertical climbing style, whereas African apes and atelids use a dorsiflexed-ankle style of vertical climbing^{11,16,25}. African apes use knuckle-walking and heel strike plantigrady when traveling quadrupedally on the ground between trees, which they climb to access food and avoid predators, and in which they construct sleeping nests^{17,18}.

As part of the ankle (talocrural) joint, the talus plays a key role in the kinematically distinct vertical climbing style employed by African apes by enabling increased dorsiflexion and inversion, which minimizes potentially lethal backwards pitching moments by positioning the center of mass closer

to the support. Vertical climbing involves hindlimb extension, including a high degree of talocrural plantarflexion, which loads the anterior side of the talocrural joint from an initially flexed hindlimb posture (Fig. 1A and SI Fig. S1, Supplementary Note 1)²⁶⁻³³. Species whose arboreal locomotor repertoire features the dorsiflexed-ankle style of vertical climbing tend to display more trapezoidal talocrural joints, whereas those of bipeds and arboreal quadrupeds tend to be more square-shaped^{25,30}. The increased mediolateral breadth of the talocrural joint is hypothesized to decrease joint stress via increased surface area³⁴. Several studies support the hypothesis that talar morphology is correlated with locomotor behavior among humans and non-human primates^{25,30,32,34-41}. However, Lovejov and colleagues¹ suggested the talus to be of limited value for inferring locomotor behavior due to high levels of variation across hominoids and described the presence of features associated with talocrural dorsiflexion in vertical climbing as "minimally expressed" (p. 72e1) in the Ar. ramidus talus (ARA-VP-6/500-023). In contrast, later qualitative assessments of the same specimen suggested a broadly ape-like morphological affinity^{37,38}. Therefore, in this study, we assessed how talar morphology tracks vertical climbing in African apes using a broad comparative sample of anthropoid primates to test whether the ARA-VP-6/500-023 talus of Ar. ramidus possessed vertical climbing features.

Results

The simplified biomechanical model described here builds on previous work^{25–31,38} (Fig. 1, Supplementary Fig. 1, Supplementary Note 1) and predicts that species whose arboreal locomotion prominently features the dorsiflexed-ankle style of vertical climbing^{21,25,30} should have, among other traits, a relatively short forefoot compared to bipeds and quadrupeds to reduce the length of the external moment arm acting on the foot and ankle

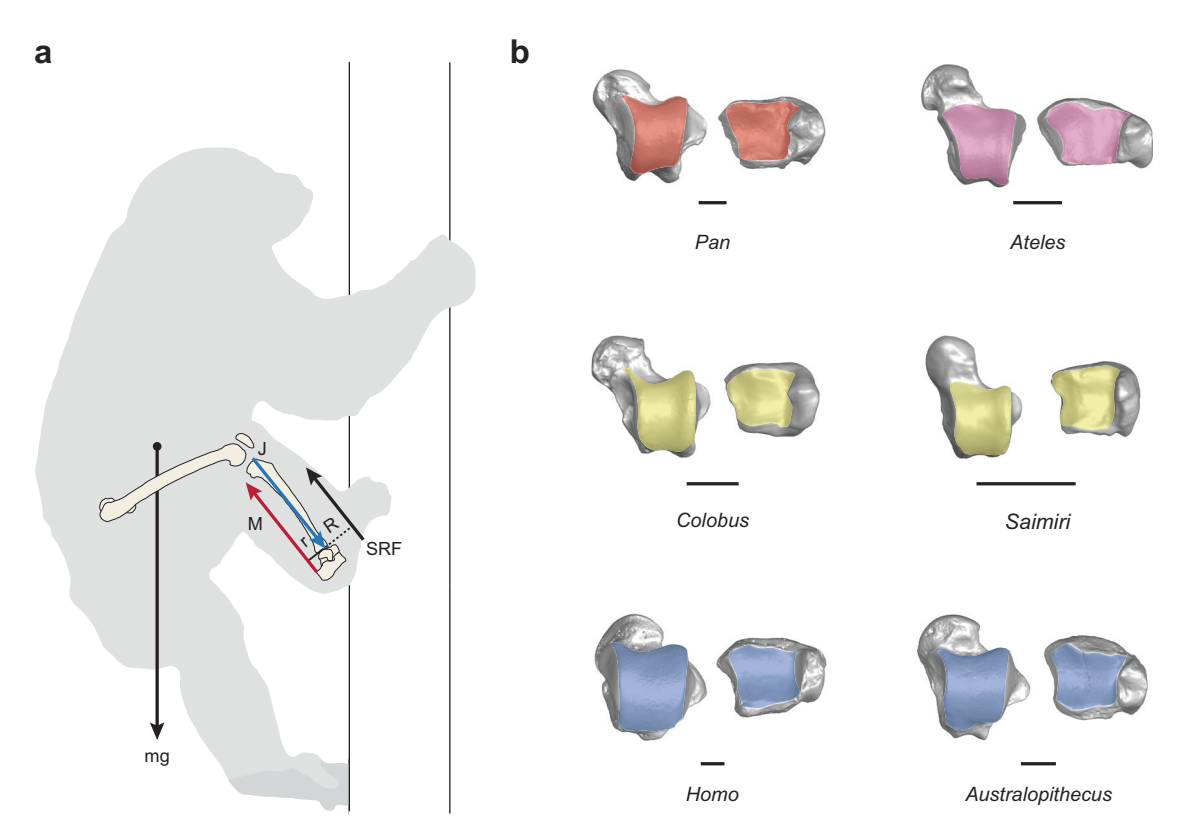


Fig. 1 | The mechanics of vertical climbing provide a proximate explanation for the convergent evolution of ankle morphology in African apes and atelids. a The silhouette displays a chimpanzee redrawn from a photograph in DeSilva^{25,30}. The simplified free-body diagram depicts hypothetical hind limb forces based on refs. 25–31,38. SRF = support reaction force, M = triceps surae muscle force, r = internal moment arm of triceps surae muscle force, R = external moment arm of the SRF, J = joint reaction force, mg = body weight vector. Magnitudes, spatial

orientations, and points of application of force vectors are hypothetical. \mathbf{b} Species whose arboreal locomotor repertoire includes high frequencies of the dorsiflexed-ankle style of vertical climbing have trapezoidal ankle shapes, whereas arboreal quadrupeds and bipeds have more square-shaped joints. Note that African apes and atelids share similar trapezoidal talocrural joint shapes, whereas arboreal quadrupeds and bipeds share more square-shaped morphologies 25,30,34 . Scale bar = 1 cm.

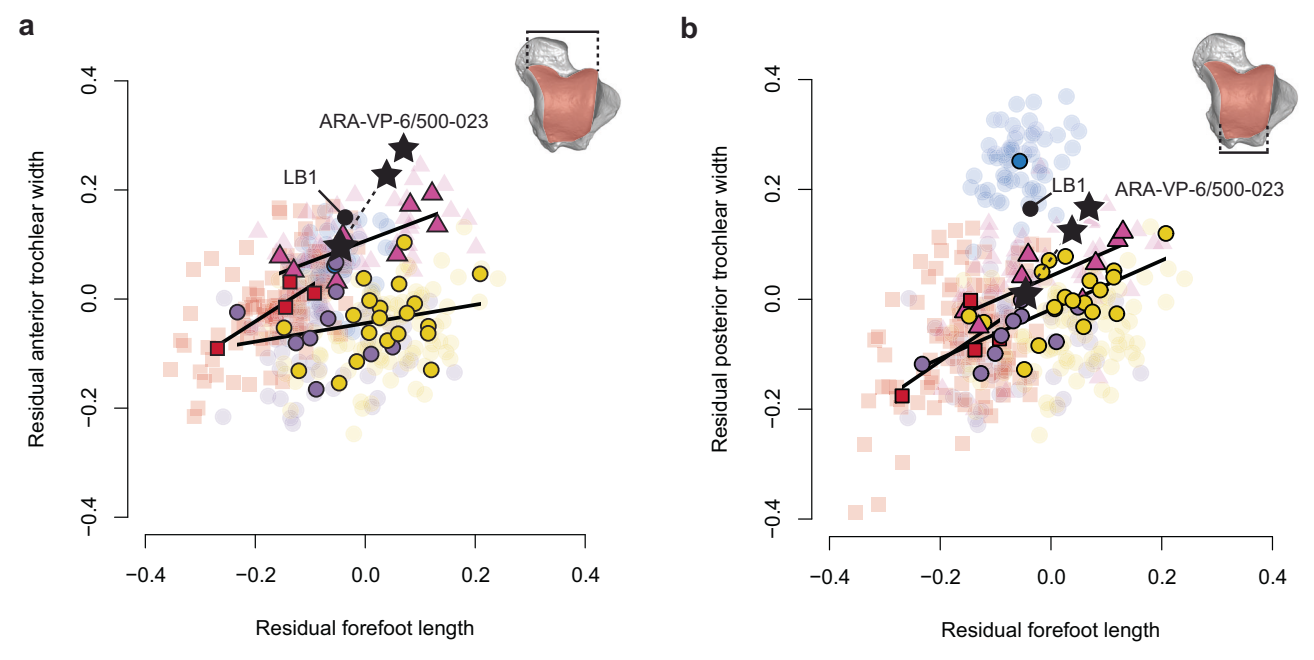


Fig. 2 | **Relative forefoot and talar dimensions. a** The relative width of the anterior trochlea as a function of the relative length of the forefoot across species means. **b** The relative width of the posterior trochlea as a function of the relative length of the forefoot across species means. Red squares = *Pan troglodytes, Pan paniscus, Gorilla gorilla, Gorilla beringei*; pink triangles = *Ateles, Alouatta, Lagothrix*; blue circles = *Homo sapiens*; purple circles = *Pongo* and hylobatids; gold circles = cercopithecoids and non-atelid platyrrhines; black circle = LB1, Liang Bua 1, *H. floresiensis*; black

stars = ARA-VP-6/500-023 (32.1, 36.2, and 51 kg body mass estimates). Transparent points indicate raw intraspecific values. Dashed lines indicate the axis describing the range of body mass estimates for ARA-VP-6/500. Note the positive correlation and higher slope of African ape and atelia anterior trochlear widths, and the relatively large posterior trochlear widths of modern humans and fossil hominins. The 3D model is ARA-VP-6/500-023 in dorsal view with the tibial facet highlighted in transparent red.

(R). We examined forefoot length (the sum of talar neck, cuboid body, and fifth metatarsal lengths⁸), and the anterior and posterior mediolateral widths of the talar trochlea as a function of estimated body mass using phylogenetic generalized least-squares regression (Supplementary Fig. 2). The forefoot lengths of Pan, Gorilla, and hylobatids are short for their estimated body masses, whereas Pongo, cercopithecoids, and non-atelid platyrrhines have the largest values. The atelid forefoot is relatively longer than those of African apes and hylobatids, but shorter than those of cercopithecoids and non-atelid platyrrhines. The human forefoot is relatively longer than those of P. troglodytes, G. gorilla, and G. beringei, but they overlap extensively with that of Pan paniscus. The cercopithecoid and non-atelid platyrrhine forefoot is relatively longer than that of humans. The relative length of the ARA-VP-6/500-023 forefoot falls at the high end of the human range of variation, which is consistent with the results of a previous study⁸.

The biomechanical model described here also predicts a positive relationship between relative forefoot length and the mediolateral width of the anterior talar trochlea among species whose arboreal locomotion prominently features the dorsiflexed-ankle style of vertical climbing because longer feet should require higher magnitude plantarflexion forces that are concentrated on the anterior surface of the trochlea. In other words, for a given body mass, African apes and atelids with relatively longer feet should display mediolaterally wider anterior talar trochleae compared to other taxa. Consistent with this prediction, African apes and atelids have stronger correlations (r = 0.91 and r = 0.74, respectively) and higher slopes (slope = 0.64, p = 0.09; slope = 0.38, p = 0.03) between the residual width of the anterior talar trochlea and residual forefoot length compared to the sampled non-human primate taxa (r = 0.25; slope = 0.17, p = 0.2, Fig. 2a). The analysis of African ape species means is underpowered because there are only four taxa sampled, which makes it difficult to obtain p-values below the 0.05 threshold. Therefore, the correlation and slope values should be interpreted cautiously for the African apes due to this uncertainty. However, the analysis of the African ape intraspecific values achieves statistical significance due to the substantially larger

sample size (n = 102, $p = 2.011^{-10}$). A future study could expand on this analysis by collecting larger samples of African ape subspecies to test the hypothesis that relative ankle dimensions are correlated with relative forefoot dimensions across populations. The evolution of a longer forefoot in humans, combined with a reliance on plantarflexion in bipedal push-off, should increase the loading of the posterior side of the talar trochlea^{25,30,38,39}. Humans therefore have a relatively wide posterior talar trochlea for their body mass and forefoot length (Fib. 2b, Supplementary Fig. 2). LB1 has a relatively wide posterior talar trochlea for its relative forefoot length compared to African apes, with larger values than most nonhuman primates that have similarly long forefeet (Fig. 2b), falling within the low end of the human range (Supplementary Fig. 2c). The anterior talar trochlea of ARA-VP-6/500-023 is wide relative to all body mass estimates, whereas the relative width of its posterior talar trochlea either falls within the overlapping distributions of P. troglodytes and H. sapiens, or within the distribution of P. troglodytes. All the relative widths of the posterior talar trochlea of ARA-VP-6/500-023 fall above the interquartile ranges of P. paniscus, G. gorilla, and G. beringei, and the largest estimates fall above all of their ranges. The A. afarensis (A.L. 288-1as) and A. sediba (U.W. 88-98) specimens also have relatively wide posterior talar trochleae for their estimated body masses that fall within the overlapping ranges of H. sapiens and P. troglodytes (Supplementary Fig. 2c). The extent to which plasticity, evolutionary adaptation, or some combination of the two explain these patterns is unclear, though talar articular morphology may not be particularly plastic compared to long bone diaphyseal properties⁴⁰.

We computed the ratio of the mediolateral width of the anterior talocrural joint to the mediolateral width of the posterior talocrural joint multiplied by 100, which we term the talar interarticular index (TII), in a large sample of extant and fossil anthropoid primates (Supplementary Table 1, Supplementary Data 1 and 2). The TII reflects the extent to which the dimensions of the talocrural joint assume a more trapezoid- or square-like configuration in dorsal view (i.e., 'wedging') following work by DeSilva^{25,30,38}. African apes, especially gorillas, have the largest TII values among

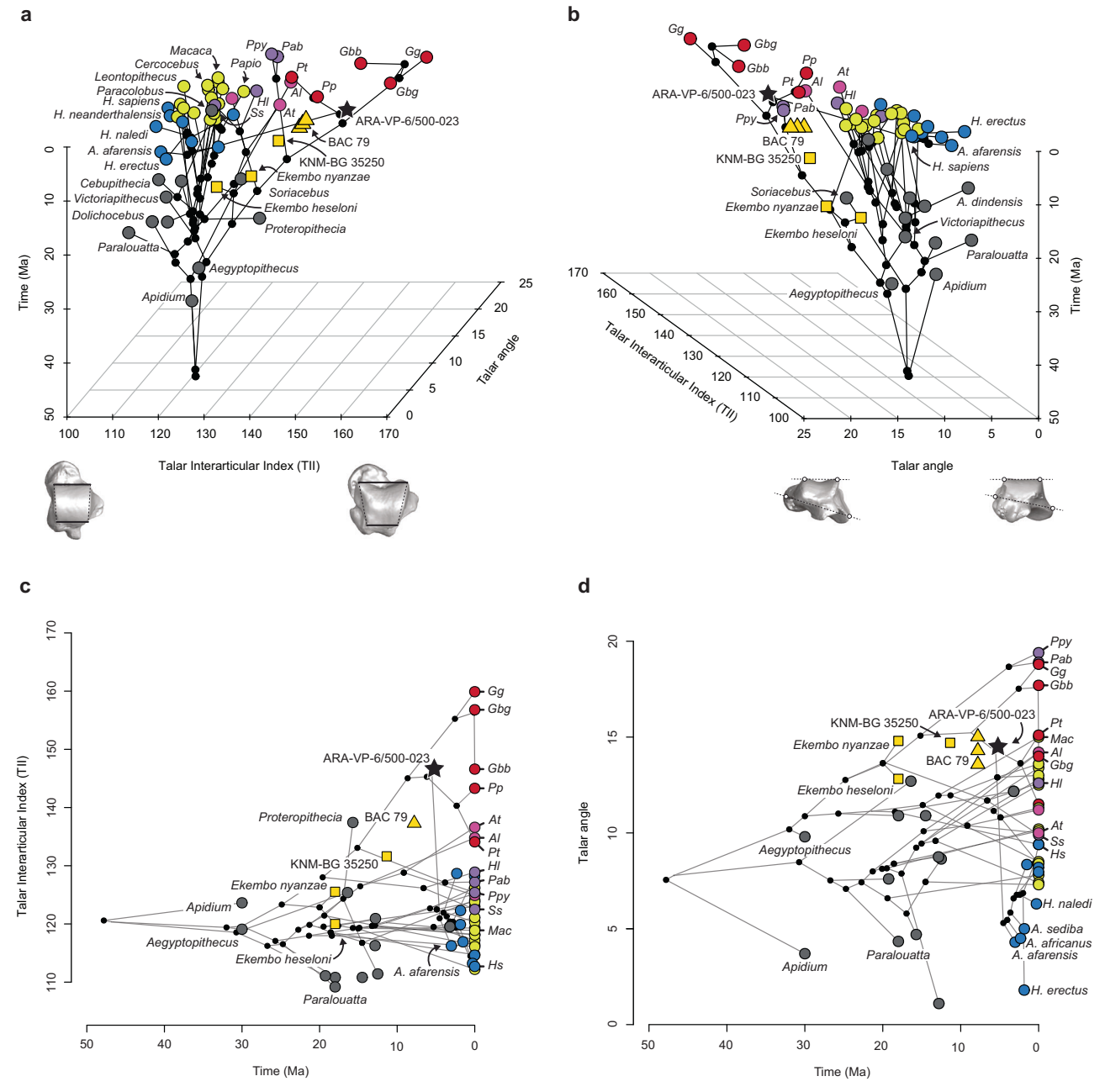


Fig. 3 | Phylomophospace plots of talocrural shape evolution in humans, apes, and monkeys. a 3D phylomorphospace plot focused on the TII with 3D models representing the range of plot values. b 3D phylomorphospace plot focused on the talar angle with 3D models representing the range of plot values. Estimated ancestral values are represented by internal nodes. A range of plausible talar angle values is displayed for BAC 79 due to damage. c 2D phylomorphospace plot for the TII. d 2D phylomorphospace plot for the talar angle. Grey circles = fossil cercopithecoids, platyrrhines, and Eocene/Oligocene anthropoids; blue circles = fossil hominins; red circles = chimpanzees and gorillas; purple circles = orangutans and hylobatids; pink circles = atelids; yellow circles = extant cercopithecoids and non-atelid platyrrhines.

Hs = Homo sapiens, Pt = Pan troglodytes, Pp = Pan paniscus, Gg = Gorilla gorilla, Gbg = Gorilla beringei graueri, Gbb = Gorilla beringei beringei, Ppy = Pongo pygmaeus, Pab = Pongo abelii, Hl = Hylobates lar, Ss = Symphalangus syndactylus, Mac = Macaca, At = Ateles, La = Lagothrix, Al = Alouatta; A. afarensis = A.L. 288-1as, A.L. 333-147; H. erectus = D4110; H. naledi = U.W. 101-1417, U.W. 101-148/149; H. neanderthalensis = Regourdou, Tabun, Krapina, La Chapelle 1, La Ferrassie 1, Spy; Nacholapithecus kerioi = KNM-BG 35250; Coropithecus bambolii = BAC 79; Ekembo nyanzae = KNM-MW 13142C, EKNM-RU 1743; Ekembo heseloni = KNM-RU 1744, EKNM-RU 1745, EKNM-RU 2036. All extant taxa are situated at time = 0.

anthropoids, whereas modern humans and cercopithecine monkeys have the smallest values (Fig. 3, Supplementary Fig. 3). There is an arboreal-terrestrial morphocline among gorillas with the largest TII values in *G. gorilla* followed by *G. beringei graueri* and *G. beringei beringei*, which is consistent with previous work^{36,39}. ARA-VP-6/500-023 has the highest TII (147) of any fossil talus included here, falling within the interquartile ranges of *P. paniscus* and *G. beringei* and within the ranges of hylobatids and *Ateles*. Other fossil

hominins have reduced TII values, most of which fall within the range of modern humans and other taxa, but among them, StW 88 (*Au. africanus*) and LB1 (*H. floresiensis*) have the highest values (~128). Miocene hominoid tali have much lower TII values that fall within the ranges of numerous anthropoid taxa, although it is noteworthy that KNM-MW 13142C (*E. nyanzae*) and the estimates for BAC-79 (*O. bambolii*) fall within the ape range.

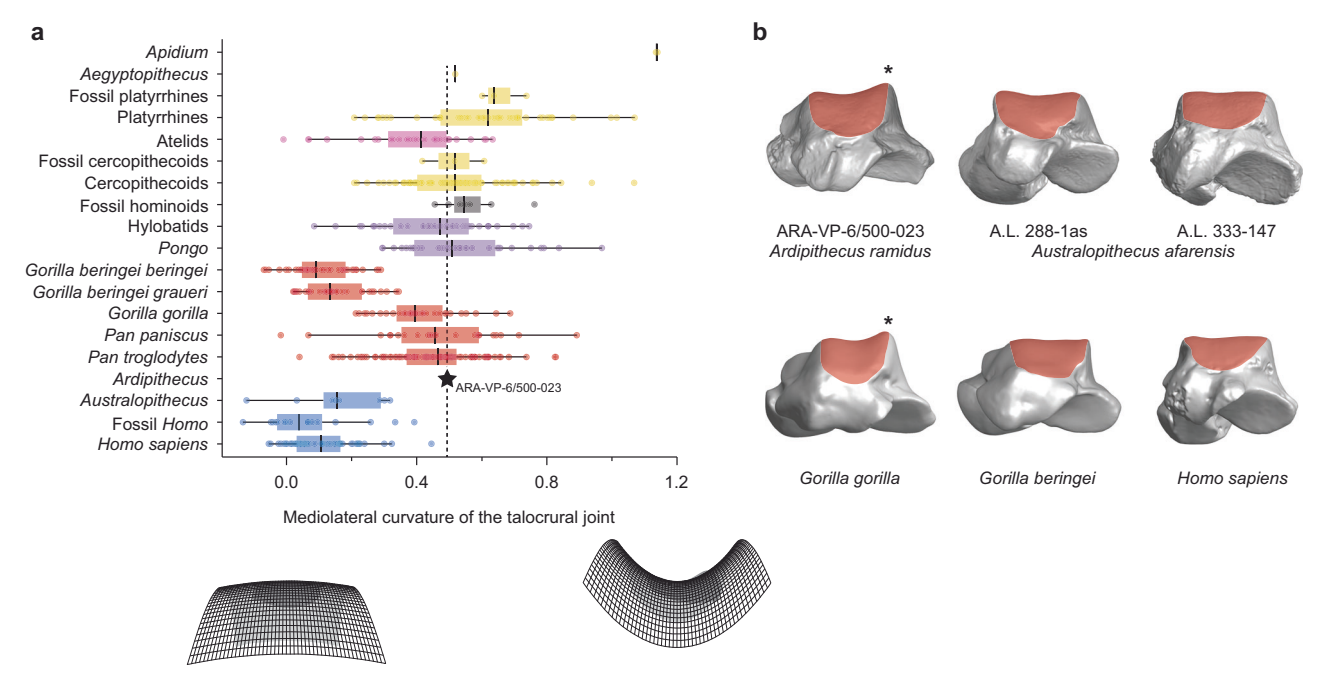


Fig. 4 | The *Ardipithecus* talus displays increased mediolateral curvature of the talocrural joint compared to other hominins. a Box and whisker plots display variation in talocrural joint curvature quantified with quadric surface fitting. The dashed vertical line indicates the value for ARA-VP-6/500-023. Quadric surfaces fit to the talocrural joint display maximum and minimum curvature values among the comparative sample. b ARA-VP-6/500-023 displays increased mediolateral

curvature and an elevated lateral trochlear rim (noted by the asterisk) similar to western lowland gorillas when compared to *Au. afarensis* (A.L. 288-1as, A.L. 333-147), modern humans, and mountain gorillas. Also note the more laterally projecting lateral malleolar facet in gorillas and ARA-VP-6/500-023, and the slightly dorsally wider, more obliquely oriented FHL groove, compared to *Au. afarensis* and modern humans, combined with well-developed rims.

The talar angle was quantified in the frontal plane using three-dimensional scans of anthropoid tali¹.25,30,32,38. The talar angle reflects the angular relationship between the talocrural joint and the long axis of the tibial diaphysis within the frontal plane²5,30,32,38. ARA-VP-6/500-023 has a talar angle of 14.5°, as reported by Lovejoy and colleagues¹, which is the largest of any known fossil hominin and falls within the ranges of most non-human primate taxa included here. The ARA-VP-6/500-023 talar angle falls within the interquartile ranges of *P. troglodytes, G. beringei, Hylobates, Macaca, Alouatta*, and callitrichids. The GWM67/P2b *Ar. ramidus* talus from As Duma (Gona Project study Area, Ethiopia) could not be included in this study, but a reconstruction of the talar head and neck with the body suggests that the talar angle could be as low as 8–10°41. All of the other fossil hominins have extremely low talar angles, most of which fall at the bottom of the human range or just below it (Fig. 3, Supplementary Fig. 4).

The evolutionary history of the anthropoid TII and talar angle was estimated using a stable model of continuous trait evolution (Fig. 3a). First, the results strongly suggest that the low TII and talar angles of most extant cercopithecoids and platyrrhines have been relatively constrained over the past ~40 million years of anthropoid evolutionary history as evidenced by low values for Apidium^{42,43} (DPC 3054, DPC 5027, DPC 5416), Aegyptopithecus⁴³ (DPC 1301, DPC 3052), Victoriapithecus⁴⁴ (KNM-MB 9422), and several other taxa, combined with estimated low ancestral values. Second, fossil apes (Ekembo nyanzae, KNM-MW 13142C⁴⁵, KNM-RU 1743^{46,47}; *Nacholapithecus kerioi*, KNM-BG 35250⁴⁸; Oreopithecus bambolii, BAC 7949) began to diverge from the ancestral anthropoid pattern toward the modern great ape condition in the Early to Middle Miocene. Third, by the Middle to Late Miocene, ARA-VP-6/500-023 and the estimated value for the Homo-Pan LCA are derived in the direction of Pan and Gorilla relative to that of most other anthropoids, consistent with a vertical climbing adaptation. Fourth, the talocrural similarities between African apes and atelids, initially highlighted by DeSilva²⁵, are most likely the result of convergent evolution. This convergence may reflect biomechanical similarities in vertical climbing^{25,29,30,33}, foot posture (i.e., heel strike plantigrady in African apes and midfoot plantigrady in atelids), or a combination of both. Finally, the *Australopithecus* ankle evolved toward smaller TII and talar angle values associated with adaptation to bipedalism in the Pliocene (Fig. 3b) due to the mediolateral expansion of the posterior trochlea^{25,30} relative to body mass (Fig. 2b, Supplementary Fig. 2c).

The mediolateral curvature of the talocrural joint was quantified using quadric surface fitting^{36,50}, which captures trochlear grooving⁵¹. The exact mechanical function of variation in trochlear depth is unknown, but the spectrum of arboreality and terrestriality is reflected in the mediolateral curvature of the talocrural joint among extant hominoids. Among extant hominoids, recent modern humans and eastern gorillas have the flattest talocrural joints, whereas orangutans and hylobatids have the greatest curvature, with chimpanzees and bonobos in between. The ARA-VP-6/500-023 talus has the highest mediolateral curvature, and therefore the deepest trochlear groove, among the fossil hominin sample (Fig. 4a), and clearly displays an African ape-like talocrural morphology in a posterior view (Fig. 4b). As noted previously, the GWM67/P2b specimen attributed to Ar. ramidus could not be included in this study, but Simpson and colleagues⁴¹ display a posterior view of the talus that demonstrates a grooved trochlear surface that is qualitatively deeper than that of ARA-VP-6/500-023 but with a slightly more elevated medial trochlear rim³⁸.

Finally, we performed multivariate analyses of overall talar shape using linear (Supplementary Fig. 5) and three-dimensional data sets to assess the morphometric affinities of the ARA-VP-6/500-023 talus (Fig. 5, Supplementary Fig. 6, Supplementary Tables 2, 3, Supplementary Data 3–6, Supplementary Results). Recent modern humans are well-separated from the other taxa (Supplementary Fig. 6a–c, Supplementary Data 3 and 5) by variables reflecting the more plantar orientation of the articular surfaces relative to the talocrural joint, a mediolaterally flatter talocrural joint, a mediolaterally wider posterior talocrural joint, a proximodistally longer and mediolaterally narrower posterior calcaneal facet, and a mediolaterally wider talar head (Fig. 5; Supplementary Data 3 and 5). Most fossil hominins are classified as 'Homo sapiens' in linear and 3D analyses, but tali of Homo floresiensis (LB1-15) and Homo naledi (U.W. 101-1417) variably display

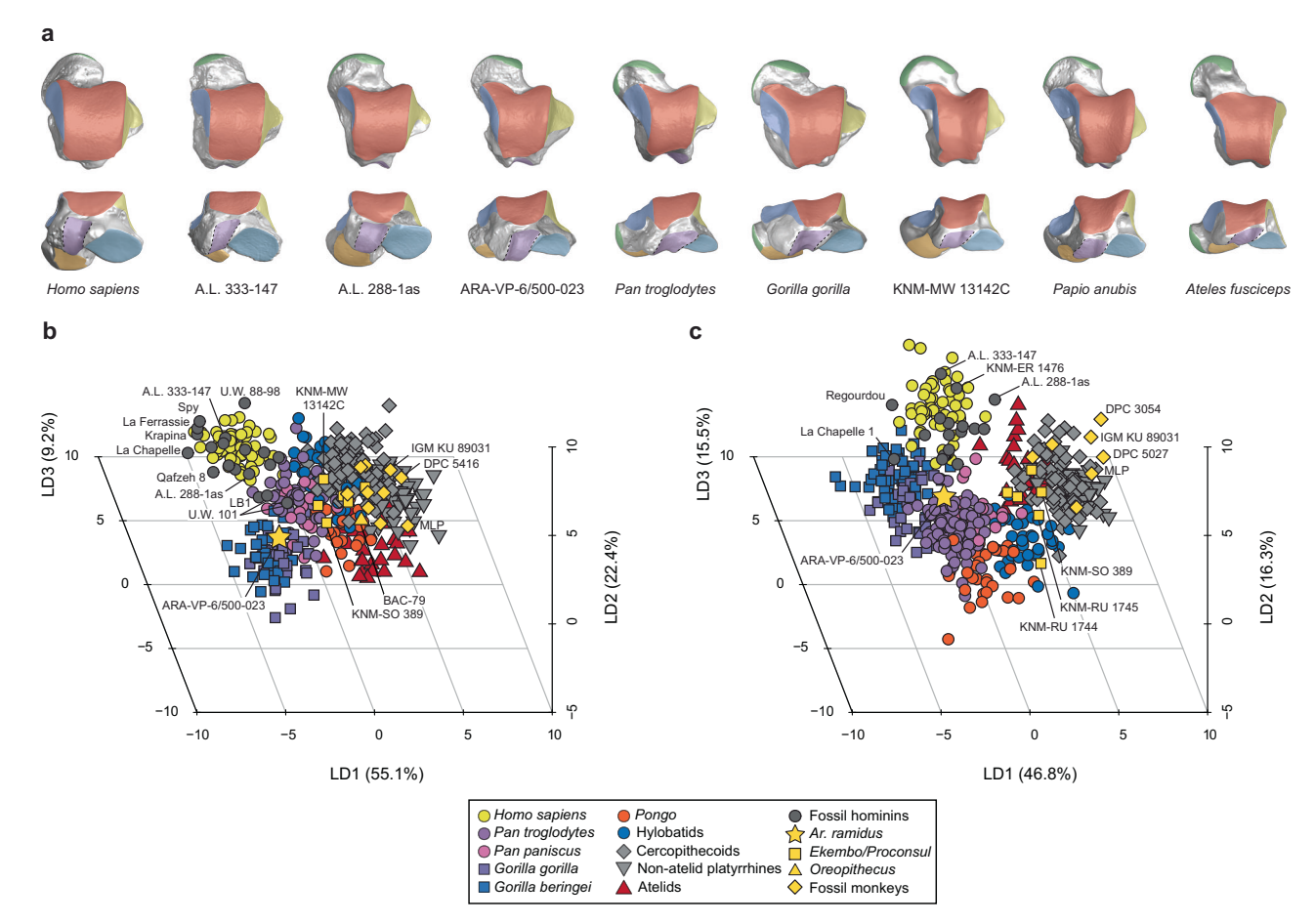


Fig. 5 | Multivariate analyses demonstrate the African ape-like affinities of the ARA-VP-6/500-023 talus. a 3D models of tali with segmented articular surfaces. Red = tibial facet, yellow = lateral malleolar facet, dark blue = medial malleolar facet, light blue = posterior calcaneal facet, green = navicular facet, orange = anterior calcaneal facet, purple = flexor hallucis longus groove. b Linear discriminant analysis on 11 geometric mean-standardized talar measurements. c Linear discriminant

analysis on 23 3D morphometric variables, including relative surface areas, proximodistal and mediolateral talocrural joint curvatures, and angles between planes fit to each surface. The ARA-VP-6/500-023 talus is classified as *Gorilla gorilla* (**b**, posterior probability = 88%) and *Pan troglodytes* (**c**, posterior probability = 74%). Note the flexor hallucis longus groove of ARA-VP-6/500-023, which is morphologically intermediate between *Pan* and A.L. 288-1as.

some affinity with African apes (Supplementary Fig. 6a, Supplementary Data 4 and 6).

Miocene fossil hominoid tali attributed to Ekembo heseloni (KNM-RU 1744, KNM-RU 1745, KNM-RU 2036)46,47, Ekembo nyanzae (KNM-RU 1743, KNM-MW 13142C)⁴⁵⁻⁴⁷, and *Proconsul major* (KNM-SO 89)^{46,47,52} are classified either as 'cercopithecoid' or 'hylobatid' (Supplementary Fig. 6d, Supplementary Data 4 and 6). Notably, the Oreopithecus bambolii (BAC-79)⁴⁹ talus is classified as 'atelid' with high posterior probability (0.97, Supplementary Data 4). The fossil cercopithecoid KNM-BC 3 (Paracolobus chemeroni)53 is classified as 'NWM' or 'Pongo' in the linear analysis (Supplementary Data 4) or 'OWM' in the 3D analysis (Supplementary Data 6). The fossil platyrrhines (UCMP 38762, Cebupithecia sarmientoi⁵⁴; IGM-KU 89031, Neosaimiri fieldsi⁵⁵; MLP 91-IX-1-119, Proteropithecia neuquenensis⁵⁶; IGM-KU 8802, Aotus dindensis⁵⁷; IGM-KU 8803, Saimiri annectens⁵⁷; MACN SC 271, Carlocebus carmenensis⁵⁸; MACN-SN 397, Soriacebus ameghinorum⁵⁸) are mostly classified as 'NWM' in both the linear and 3D analyses (Supplementary Data 4 and 6). The Eocene/ Oligocene anthropoids (DPC 3054, DPC 5027, DPC 5416, Apidium phiomense^{42,43}; DPC 1301, Aegyptopithecus zeuxis⁴³) are classified as 'NWM' in both analyses.

The ARA-VP-6/500-023 talus is classified as 'Pan troglodytes' (posterior probability = 0.74) in the 3D analysis and 'Gorilla gorilla' in the linear analysis (posterior probability = 0.88, Supplementary Data 4 and 6). In the 3D analysis, the ARA-VP-6/500-023 talus falls at one end of the multivariate axis separating African apes from recent modern humans. Inspection of the

variable loadings and the distributions of individual variables included in the 3D multivariate analysis (Supplementary Figs. 5–11) shows that, compared to most African apes in our sample, the ARA-VP-6/500-023 talus tends to have a reduced relative area of the navicular facet (Supplementary Fig. 7f), an increased relative area of the posterior calcaneal facet (Supplementary Fig. 7b), a larger angle between the anterior calcaneal and posterior calcaneal facets (Supplementary Fig. 8c), and a larger angle between the anterior calcaneal and medial malleolar facets (Supplementary Fig. 11b).

Our comprehensive morphometric analysis demonstrates that the ARA-VP-6/500-023 talus displays a predominantly African ape-like talar morphology, particularly related to talocrural joint shape and orientation. Moreover, with subtle modifications to its anterior subtalar joint, the ARA-VP-6/500-023 talus is slightly more similar to those of other hominins than African apes in the 3D LDA (Fig. 5c). Additionally, a series of non-metric features further reflect a mosaic talar morphology in ARA-VP-6/500-023 (Supplementary Fig. 12). Specifically, although the ARA-VP-6/500-023 talus shares clear metric (Fig. 5) and non-metric similarities with African apes (Supplementary Fig. 12a), it is characterized by a hominin-like extension of the talocrural articular surface proximally combined with a deep, proximally positioned, flexor hallucis longus (FHL) groove due the development of its medial rim. Additionally, the ARA-VP-6/500-023 talus displays a bifurcated anterior calcaneal facet with distinct proximal and distal segments (Supplementary Fig. 13). Consequently, the distal segment of the anterior calcaneal facet forms a planar articular extension beneath the talar head, which would be positioned dorsally relative to the cuboid facet. In

contrast, Miocene hominoids are characterized by a combination of apeand monkey-like features (Supplementary Fig. 12c).

Discussion

Our morphometric analyses demonstrate that the talar morphology of ARA-VP-6/500-023, unlike all sampled fossil specimens representing approximately 40 million years of evolutionary history, shares affinities with African apes. Our ancestral estimations suggest that the talar morphology shared by ARA-VP-6/500-023, Pan, and Gorilla, and on which atelids converge to some degree^{25,30,33}, is derived relative to that of fossil apes, fossil monkeys, and Eocene/Oligocene anthropoids. Although there are many outstanding questions about the mechanistic effects of talar form on foot function in humans, apes, and monkeys⁵⁹, we interpret these shared aspects of talar morphology to reflect adaptation to terrestrial plantigrade quadrupedalism²¹ and the dorsiflexed-ankle style of vertical climbing^{25,30} in the Homo-Pan LCA and early fossil hominins such as Ar. ramidus. Our quantitative analysis supports earlier qualitative observations of a more apelike morphology of the ARA-VP-6/500-023 talus^{37,38} than originally suggested^{1,2}. However, the ARA-VP-6/500-023 talus is not entirely African ape-like because it displays hominin-like modifications of the subtalar and talocrural joints, and FHL groove (Figs. 2, 5). Collectively, these results are inconsistent with human and chimpanzee evolution from a generalized arboreal ancestor that lacked adaptations for terrestrial quadrupedalism, vertical climbing, and suspension^{1-3,5}.

The extent to which talar morphology reflects function or phylogeny has been debated^{1,25,35,36,39,40,59}. A study by Nozaki and colleagues⁵⁹ argued that talar morphology is more phylogenetically conserved, rather than functionally informative, in non-human primates because chimpanzees and western lowland gorillas display differences in 3D talus shape despite sharing similar locomotor repertoires⁵⁹. Turley and Frost³⁵ found that locomotion explained the highest proportion of variation in the 3D shape of the talus in a large comparative sample, followed by body size and phylogeny. Similarly, Monclús-Gonzalo and colleagues⁴¹ found that locomotor behavior is significantly correlated with the 3D shape of the talus across hominoids, cercopithecoids, and platyrrhines. Recent studies focusing on variation within and between Pan and Gorilla have shown that talar morphology predictably reflects ecology and locomotion^{36,39,40}. Our analysis showed that the more terrestrial G. beringei has a reduced TII (Fig. 2, Supplementary Fig. 3), talar angle (Fig. 2, Supplementary Fig. 4), anterior trochlea width (Fig. 3, Supplementary Fig. 2), and mediolateral curvature of the talocrural joint (Fig. 4) compared to more arboreal G. gorilla. These analyses are consistent with the hypothesis that talar morphology reflects locomotor behavior among large-bodied, closely related African ape species^{25,30,32,36,39,40}. Therefore, the talar similarities between ARA-VP-6/500-023, G. gorilla, and P. troglodytes (Figs. 2-5), along with their differences from the more terrestrial G. beringei and more arboreal Pongo, imply that both vertical climbing and terrestriality were significant components of the positional repertoire of Ar. ramidus.

Overall, we interpret the mosaic morphology of the ARA-VP-6/500-023 talus to reflect a combination of African ape-like vertical climbing as part of a varied positional repertoire that included orthograde posture, forelimb-dominated suspensory locomotion, and an early form of bipedalism (Supplementary Fig. 12). The relatively high talar angle of ARA-VP-6/ 500-023 compared to other fossil hominins does not, in isolation, support a vertical climbing hypothesis due to the overlap across taxa that use different locomotor modes, but it may indicate the retention of a more African apelike ankle posture relative to other fossil hominins¹. The 'total morphological pattern' of the ARA-VP-6/500 partial skeleton supports the hypothesis that the positional repertoire of the earliest hominins included vertical climbing and suspension. In a previous study, the hand shape of Ar. ramidus was placed in a selective regime with chimpanzees and bonobos, implying shared adaptation to orthogrady, below-branch suspension, and vertical climbing⁹. The ARA-VP-6/500 foot has an elongated first metatarsal relative to the length of the fifth metatarsal, which is argued to increase the moment arm of the intrinsic hallucal adductor musculature (e.g., m. adductor

hallucis), and reflects the forceful hallucal grasping characteristic of African apes associated with vertical climbing ^{6,60,61}. The pelvis of *Ar. ramidus* displays an elongated ischium³, which suggests a greater capacity to produce hip extension moments in vertical climbing compared to later hominins ⁶². The foot proportions of *Ar. ramidus* are most similar to heel strike plantigrade gorillas ⁶³ when examined relative to a foot geometric mean ⁶ or a postcranial geometric mean representing the preserved size of the ARA-VP-6/500 partial skeleton ⁸.

We focus on the vertical climbing features of the talus to address current debates about the locomotion of Ar. ramidus and the Homo-Pan LCA^{1,6,8,25,30,37,38}, but the talar morphology of African apes likely reflects multiple factors, including large body mass, phylogeny, and their unique combination of climbing and terrestrial plantigrade quadrupedalism^{21,25,3} 35,36,39,40,59,63. A laboratory analysis of 3D marker-based foot and ankle kinematics demonstrated the use of talocrural dorsiflexion during climbing, arboreal quadrupedalism, and terrestrial quadrupedalism in chimpanzees³³. Another study on the 2D quadrupedal kinematics of captive primates also showed that chimpanzees (and gorillas) use talocrural dorsiflexion during terrestrial quadrupedalism⁶⁴, which is their most frequent locomotor mode during adulthood ^{17,19-21}. However, both studies support the hypothesis that the chimpanzee talocrural joint experiences increased dorsiflexion during vertical climbing^{25,30}. Furthermore, the shared aspects of talar morphology among African apes and atelids support the hypothesis of a convergent adaptation most plausibly explained by vertical climbing^{25,29,30,33} given the lack of terrestriality and heel strike plantigrady among the latter 63,64. Previous studies have argued that the presence of a flaring lateral malleolar facet and a more plantarly oriented talar head in African ape tali are features reflecting terrestrial plantigrade quadrupedalism^{63,65}, both of which are found in ARA-VP-6/500-023 but absent among atelid platyrrhines. Therefore, the African ape-like foot of Ar. ramidus, including the morphology of the talus, suggests that the Homo-Pan LCA had a positional repertoire that included terrestrial plantigrade quadrupedalism and vertical

Concurrently, other features of the ARA-VP-6/500 skeleton indicate that Ar. ramidus used a form of bipedalism that included basicranial reorganization⁴, the presence of an anterior inferior iliac spine on the ilium³, dorsally domed lateral metatarsal heads⁷, a more plantar-lateral position of the os peroneum sesamoid bone of the m. fibularis longus tendon¹, and a more extrinsically elongated forefoot attributed to distal tarsal length^{1,8}. The more hominin-like lateral side of the ARA-VP-6/500 foot is hypothesized to have improved lateral push-off performance compared to that of apes^{1,38}. At the same time, on the medial side of the foot, the ARA-VP-6/500-089 first metatarsal displays Gorilla-like extensions of articular surface on the dorsal side of the head (non-subchondral isthmus), it lacks dorsal doming of the head, and the ARA-VP-6/1000 second metatarsal displays paired rugosities on the dorsal side of the base for the cuneiform-metatarsal ligaments¹. The presence of an abducted hallux indicates that medial push-off must have differed from the condition inferred for Australopithecus and these medial metatarsal features imply habitual frontal plane rotation at the metatarsophalangeal joints during facultative bipedalism with an abducted hallux^{1,38}.

Although exact mechanical interpretations remain challenging based only on the traits observed in the fossil record, we hypothesize that the lateral extension of the anterior calcaneal facet (Supplementary Fig. 13) reflects a modified articular relationship of the talus and calcaneus in ARA-VP-6/500-023 relative to those of apes. This morphology may indicate the use of an everted transverse tarsal joint during the stance phase of facultative bipedalism in *Ar. ramidus*, with the talar head buttressed against the dorsal side of the calcaneocuboid joint. A 3D kinematic study on chimpanzees showed that terrestrial quadrupedalism involves more everted transverse tarsal joint postures compared to the more inverted postures used during climbing³³. Notably, this observation is consistent with the morphology of the preserved distal calcaneus from As Duma (Gona Project study area, Ethiopia) attributed to *Ar. ramidus* (GWM67/P2c), which displays an anterolateral process and a lateral extension of the anterior talar facet dorsal to the cuboid facet⁴¹. Furthermore, the talar angle of GWM67/P2b from As

Duma may be more derived than that of ARA-VP-6/500-023^{38,41}, which could reflect population-level variation in *Ar. ramidus* necessary for the selection of traits that would improve bipedal performance.

The more hominin-like proximal extension of the flexor hallucis longus (FHL) groove might imply that the extrinsic digital flexor musculature could have exerted a larger magnitude plantarflexion moment at the ankle during bipedal push-off⁶⁶. The observation of an elongated forefoot and the potential for a relatively wide posterior talar trochlea, in ARA-VP-6/ 500-023, is consistent with this functional hypothesis. However, the ARA-VP-6/500-023 FHL groove is also deep, mediolaterally wide dorsally, and its lateral rim is more obliquely oriented relative to the talocrural axis of rotation and therefore more similar to the African apes than to other fossil hominins³². Functionally, these features suggest greater muscle size and possibly greater force production during contraction for hallucal grasping or for counteracting extension moments on the digits during the stance phase of terrestrial locomotion. Therefore, we interpret the functional morphology of the ARA-VP-6/500-023 talus to be consistent with a positional repertoire that included African ape-like vertical climbing and early bipedalism. Outstanding questions concerning the frequency and biomechanics of terrestrial bipedalism in Ardipithecus are important, but we cannot address them with our dataset.

Keith⁶⁷ was among the earliest to suggest that humans and chimpanzees evolved from an ancestor with a body plan adapted to hominoid-like orthogrady rather than monkey-like pronogrady. Building on Keith's hypothesis, others suggested that humans evolved from a suspensory ('brachiating') ancestor, which resulted in decades of research on the anatomical requisites of suspensory positional behavior and debates about the LCA (reviewed in ref. 10). However, in the 1970s, an alternative hypothesis emerged from a synthesis of behavioral observations, comparative anatomy, and biomechanics in which the locomotor precursor to hominin bipedalism, and the adaptive signal in the anatomy of hominoids, was not brachiation sensu stricto but a form of climbing (variably termed vertical climbing, cautious climbing, cautious quadrupedalism, or quadrumanous climbing^{68–72}). We view the African ape morphotype as a reflection of an evolutionary history characterized by orthogrady, climbing, and forelimb suspension. Therefore, climbing hypotheses 68,71,72, and hints of a climbing ancestry in the functional anatomy of hominins and apes, are not mutually exclusive with the hypothesis of an African ape-like ancestor of humans and chimpanzees 10,21,73.

Keith's multistage model proposed a "troglodytian" stage of hominoid evolution characterized by larger body mass⁶⁷. The positional repertoires of extant primates are closely tied to variation in body mass because mass is one of the main constraints on the biomechanics of animal locomotion 74,75. Most Miocene hominoids display morphological dimensions and estimated body masses that are larger than most extant non-hominids, including the atelids to which they are frequently compared, overlapping with siamangs, terrestrial baboons, and Asian colobines⁷⁶. In the absence of baboon-like terrestrial adaptations among Miocene hominoids (e.g., short pedal phalanges, digitigrade foot postures), and long external tails that could be used as balancing organs⁷⁷, their relatively large body masses necessitate modified arboreal biomechanics compared to smaller extant cercopithecoids and platyrrhines. The combination of lower TII values with higher talar angles among Miocene apes, especially the atelid- and orangutan-like morphology of BAC-79 (O. bambolii)⁴⁹, is consistent with this hypothesis. Ardipithecus ramidus, like other early hominins, was larger-bodied compared to most Miocene hominoids and extant non-hominid primates^{2,78}. Therefore, the African ape-like vertical climbing style inferred for Ar. ramidus is consistent with its large body mass estimates, talar morphology, and other aspects of its postcrania.

The fossil and comparative evidence can be used to test the null hypothesis that the *Homo-Pan* LCA was African ape-like in morphology and inferred positional repertoire¹⁰. The African ape positional repertoire is reflected in the morphology of their appendicular and axial skeletons, as well as their overall large body masses^{10,21,37,67}. At present, it is difficult to reject the null hypothesis that humans evolved from an African ape-like LCA based on

the postcranial morphology of *Ar. ramidus* and other early hominins¹⁰. The hands and feet of *Ar. ramidus*, as well as its skeletal size and body mass estimates, show clear similarities to the African apes^{1,6,8,9,78}. The postcranial morphology of *Ar. ramidus* and other early fossil hominins strongly suggests that humans evolved from a large-bodied, orthograde (short-backed) ancestor with adaptations for vertical climbing, suspension, and heel-strike plantigrady^{6,8–10,63,73,78–82}. Alternative hypotheses of a more generalized LCA without specific African ape-like adaptations^{1–3,5,83}, or an LCA with arboreal bipedal adaptations^{84,85}, are currently unsupported by the available fossil and comparative evidence^{6,8–10,79,82,86}.

The phylogenetic position of humans within the African ape clade implies evolution from an ancestor that used terrestrial plantigrade quadrupedalism, vertical climbing, and below-branch suspension. The functional morphology of *Ar. ramidus* hands and feet, including the ARA-VP-6/500-023 talus, is consistent with this hypothesis, while also displaying features plausibly associated with an early form of bipedalism. The integrative analysis of extant African ape and early fossil hominin morphology provides our best chance for making inferences about the positional repertoire of the *Homo-Pan* LCA in lieu of an African ape fossil record. Our inferences regarding the positional repertoire of *Ar. ramidus* refocus evolutionary explanations for the origin of bipedalism and, therefore, the emergence of the human lineage.

Methods

This study uses four overlapping data sets (with different sample sizes and species compositions) consisting of linear distances collected on anthropoid tali; two-dimensional talar angles collected from three-dimensional surface scans; three-dimensional joint curvatures, relative surface areas, and angles between surfaces also measured on 3D scans; and linear measurements of the cuboid, fifth metatarsal, and femoral head superoinferior diameter for quantifying forefoot length relative to estimated body mass. Linear data were collected on extant anthropoid tali housed at the following institutions (Supplementary Data 1): American Museum of Natural History; United States National Museum of Natural History; Harvard Museum of Comparative Zoology; Royal Museum for Central Africa; Cleveland Museum of Natural History; Stony Brook University; Museum of Vertebrate Zoology, University of California, Berkeley; Human Evolutionary Research Center, University of California, Berkeley; Phoebe A. Hearst Museum of Anthropology, University of California, Berkeley; Center for the Study of Human Origins, New York University. Additional anthropoid tali were downloaded from Morphosource to supplement the initial dataset (https://www. morphosource.org/), which initially appeared in ref. 87.

The fossil sample includes data from original specimens, except in a few cases where measurements were taken on casts (Supplementary Data 2). Data were collected on fossil tali of extinct hominin, hominoid, cercopithecoid, and platyrrhine taxa housed at the following institutions: National Museum of Ethiopia; Nairobi National Museum; Evolutionary Studies Institute, University of the Witwatersrand; Duke Lemur Center, Division of Fossil Primates; University of California Paleontology Museum; Museo Geologico, INGEOMINAS, Bogota, Colombia; Museo de La Plata, Argentina; Museo Argentino de Ciencias Naturales. As with the extant specimens, additional fossil platyrrhine tali were downloaded from Morphosource to supplement the fossil talus dataset.

Linear measurements were collected on tali using digital calipers: (1) talar length, (2) trochlear length, (3) talar width, (4) mediolateral width of the anterior trochlea, (5) mediolateral width of the posterior trochlea, (6) fibular facet height, (7) medial malleolar facet height, (8) mediolateral head width, (9) dorsoplantar head height, (10) mediolateral width of the posterior calcaneal facet, (11) proximodistal length of the posterior calcaneal facet (Supplementary Fig. 5). Talar length (1) is defined as the maximum proximodistal distance between the most proximal margin of the talar trochlea and the most distal point of the talar head. Trochlear length (2) is defined as the maximum proximodistal distance between the most proximal margin of the talar trochlea and the most distal point of the talar trochlea. Talar width (3) is defined as the maximum mediolateral distance between the

distolateral edge of the fibular facet and the most medial point on the talar head. Mediolateral width of the anterior trochlea (4) is defined as the mediolateral distance between the distolateral edge of the anterior talar trochlea and the distomedial margin that separates the trochlea from the medial malleolar facet. Mediolateral width of the posterior trochlea (5) is defined as the mediolateral distance between the most proximolateral corner of the fibular facet-posterior talar trochlear margin and the most proximodistal corner of the medial malleolar facet-posterior talar trochlear margin. Fibular facet height (6) is defined as the maximum dorsoplantar distance between the most plantar point of the fibular facet articular surface and the most dorsal point on the lateral margin of the talar trochlea. Medial malleolar facet height (7) is defined as the maximum dorsoplantar distance between the most plantar point of the medial malleolar articular surface and the most dorsal point on the medial margin of the talar trochlea. Mediolateral head width (8) is defined as the maximum mediolateral width of the talar head taken parallel to the long axis of the talonavicular joint. Dorsoplantar head height (9) is defined as the maximum dorsoplantar height of the navicular facet taken perpendicular to the long axis of the talonavicular joint. Mediolateral width of the posterior calcaneal facet (10) is defined as the maximum mediolateral width of the posterior calcaneal facet taken perpendicular to the long axis of the joint. Proximodistal length of the posterior calcaneal facet (11) is defined as the maximum proximodistal length of the posterior calcaneal facet articular surface taken parallel to the long axis of the joint.

Talar measurements 4 and 6 were used to derive a variable that we term the talar interarticular index (TII, [mediolateral width of the anterior trochlea/mediolateral width of the posterior trochlea]×100). Increased TII values are associated with a more wedge-shaped talocrural joint, whereas lower values are associated with a more square-shaped talocrural joint 25,30,38 .

Forefoot length was quantified as the sum of talar neck length (derived by subtracting talar trochlea length from talar length), dorsal non-articular length of the cuboid, and fifth metatarsal length (given the preservation of elements in the ARA-VP-6/500 partial foot) following Prang^{8,9}. The body mass of each individual was estimated using species-specific regression equations for humans⁸⁸, chimpanzees, gorillas, orangutans, and hylobatids⁸⁹, and the remaining non-hominoid taxa⁹⁰. Body mass estimates for fossil hominins (ARA-VP-6/500-023, A.L. 288-1, LB1, U.W. 88-98) and fossil apes (KNM-RU 2036, KNM-BG 35250) were taken from published sources^{2,78,88-93}. Lovejoy and colleagues² estimate a body mass of 51 kg for ARA-VP-6/500 based on capitate and talus measurements. Grabowski and colleagues⁷⁸ estimate body masses of 32.1 kg and 29.1 kg for ARA-VP-6/500 and MH2 (U.W. 88-98), respectively, whereas Ruff and colleagues⁸⁸ estimate body masses of 36.2 and 41 kg for these individuals. A later study by Grabowski and colleagues⁹² estimated a body mass of 50.2 kg for ARA-VP-6/ 500 using a human model. Body mass estimates range from 13.4 to 17.2 kg for KNM-RU 2036 based on first metatarsal dimensions⁹³. We therefore use four body mass estimates for ARA-VP-6/500 and two body mass estimates for U.W. 88-98 (MH2) and KNM-RU 2036. Phylogenetic generalized leastsquares regression (pGLS)94 was used to individually regress the natural logarithms of forefoot length, anterior trochlear width, and posterior trochlear width as response variables against the natural logarithm of estimated body mass. The branch lengths of the phylogeny were transformed using Pagel's lambda⁹⁵, which was estimated with a maximum likelihood procedure implemented in the 'caper' package v. 1.0.3% in R v. 4.4.0%. All response variables are in units of millimeters, and the body mass estimates are in units of kilograms prior to logarithmic transformation.

The talar angle was quantified following refs. 1,25,30,32. The talar angle (also known as the talocrural joint angle) is defined as the frontal plane angle formed between a line drawn through the most dorsal points on the lateral and medial talar trochlea rims and a second line drawn through the most plantar points on the medial malleolar and fibular facets taken in posterior view. We used Geomagic Studio software to place 3D point features on each specimen (most dorsal point on the medial trochlear rim, most dorsal point on the lateral trochlear rim, most plantar point on the medial malleolar facet,

most plantar point on the fibular facet). Then, we oriented each specimen in posterior view, enabled 3D mesh transparency to visualize the position of each point feature, and measured the talar angle from a screen capture using ImageJ software⁹⁸. Lovejoy and colleagues¹ report a value of 14.5° for the talar angle of the ARA-VP-6/500-023, which we included in subsequent analyses.

The 3D data set consists of metrics quantified on 3D scans of tali generated using a NextEngine Desktop 3D scanner. Tali were scanned in at least two orientations and merged using ScanStudio Pro Software. The resulting triangular meshes were imported into Geomagic Studio software to clean imperfections (e.g., filling small holes). Angles between surfaces were quantified by fitting least-squares planes to virtually segmented articular surfaces in Geomagic Studio, and calculated as the inverse cosine of the dot product of the normal vectors between each plane⁹⁹. Relative surface areas were quantified by dividing the surface area of the virtually segmented articular surfaces by the total bone surface area multiplied by 100¹⁰⁰. Finally, mediolateral and proximodistal curvatures of the tibiotalar surface were quantified by fitting quadric surfaces to virtually segmented tibial facets using custom software^{36,50}.

We estimated ancestral values for the talar angle and TII for a subset of our extant sample using a stable model of continuous trait evolution implemented in StableTraits software v. 1.5101 following refs. 6,8,9. StableTraits uses a Markov chain Monte Carlo (MCMC) approach that estimates the posterior distribution of ancestral states given a dataset and phylogeny while relaxing assumptions of neutrality and gradualism¹⁰¹. We ran two independent MCMC chains for 5,000,000 iterations each at a thinning rate of 200, resulting in 25,000 samples each. We used the default priors on the evolutionary rate to prevent rates from approaching zero. A proportional scale reduction factor (PSRF) value of 1 indicated chain convergence after 2,500,000 iterations, which we discarded as burn-in. We used a molecular consensus phylogeny from the 10k trees website¹⁰² with fossil taxa added in Mesquite software v. 3.81¹⁰³. The ages and phylogenetic positions of the fossil taxa were based on refs. 104–112. We excluded the fossil hominoids Oreopithecus bambolii and Nacholapithecus kerioi from the phylogeny, and therefore the ancestral estimations, because their phylogenetic positions are debated^{111,112}. Ancestral estimates and taxon mean values were visualized in a 3D phylomorphospace plot using custom code based on the 'phylomorphospace3d' function in the 'phytools' package v. 2.1^{113} in R^{97} .

We transformed our original 11 linear measurements to Mosimann shape variables by dividing each measurement by the combined geometric mean of all measurements per individual for multivariate analyses ¹¹⁴. We used linear discriminant analysis (LDA) on the pooled covariance matrix of 11 linear measurement shape variables, followed by an LDA on the pooled covariance matrix of 23 3D scale-free variables (relative surface areas, angles, and curvatures), with groups defined by taxon to determine (1) whether multivariate talus shape distinguishes such groups and (2) to which group the *Ar. ramidus* talus is most similar. We assessed the effectiveness of the LDA by evaluating the posterior probabilities of group membership for extant taxa using a leave-one-out cross-validation approach. All fossil specimens were added to the analyses a posteriori without group membership identified.

Statistics and reproducibility

The sizes of the human and nonhuman primate samples vary across the following analyses included in this study: talar angle analysis, N=384; linear discriminant analysis of linear dimensions, N=473; linear discriminant analysis of relative surface areas, angles between surfaces, and articular surface curvatures, N=503; relative foot and ankle dimensions, N=359. A complete list of all extant specimens and their accession numbers can be found in Supplementary Data 7. Sample means and standard deviations are reported for univariate metrics (i.e., talar angle, TII, and talocrural ML curvature). Phylogenetic generalized least-squares and ordinary least-squares regressions were used for the analysis of the relative size and scaling of foot and ankle dimensions, which test the null hypothesis that the

response variable is random with respect to the predictor variable. Ancestral states for the talar angle and TII were reconstructed using a Markov chain Monte Carlo (MCMC) approach using a stable model of trait evolution and a phylogenetic tree. Linear discriminant analysis was used to assess cross-validated posterior probabilities of group membership among extant taxa and the predicted group membership of fossils. All data used in the analysis are available on the Figshare digital data repository.

Reporting summary

Further information on research design is available in the Nature Portfolio Reporting Summary linked to this article.

Data availability

All data used in this analysis are available on the Figshare digital data repository (https://doi.org/10.6084/m9.figshare.26069590).

Received: 26 June 2024; Accepted: 11 August 2025; Published online: 15 October 2025

References

- Lovejoy, C. O., Latimer, B., Suwa, G., Asfaw, B. & White, T. D. Combining prehension and propulsion: the foot of *Ardipithecus ramidus*. *Science* 326, 72–72e8 (2009).
- Lovejoy, C. O., Suwa, G., Simpson, S. W., Matternes, J. H. & White, T. D. The great divides: Ardipithecus ramidus reveals the postcrania of our last common ancestor with African apes. Science 326, 100–106 (2009).
- Lovejoy, C. O., Suwa, G., Spurlock, L., Asfaw, B. & White, T. D. The pelvis and femur of *Ardipithecus ramidus*: the emergence of upright walking. *Science* 326, 71–71e6 (2009).
- Kimbel, W. H., Suwa, G., Asfaw, B., Rak, Y. & White, T. D. Ardipithecus ramidus and the evolution of the human cranial base. Proc. Natl Acad. Sci. USA 111, 948–953 (2014).
- White, T. D., Lovejoy, C. O., Asfaw, B., Carlson, J. P. & Suwa, G.
 Neither chimpanzee nor human, *Ardipithecus* reveals the surprising ancestry of both. *Proc. Natl Acad. Sci. USA* 112, 4877–4884 (2015).
- Prang, T. C. The African ape-like foot of Ardipithecus ramidus and its implications for the origin of bipedalism. eLife 8, e44433 (2019).
- 7. Fernández, P. J. et al. Evolution and function of the hominin forefoot. *Proc. Natl Acad. Sci. USA* **115**, 8746–8751 (2018).
- Prang, T. C. New analyses of the Ardipithecus ramidus foot provide additional evidence of its African ape-like affinities: a reply to Chaney et al. (2021). J. Hum. Evol. 164, 103135 (2022).
- Prang, T. C., Ramirez, K., Grabowski, M. & Williams, S. A. *Ardipithecus* hand provides evidence that humans and chimpanzees evolved from an ancestor with suspensory adaptations. *Sci. Adv.* 7, eabf2474 (2021).
- Williams, S. A., Prang, T. C., Russo, G. A., Young, N. M. & Gebo, D. L. African apes and the evolutionary history of orthogrady and bipedalism. Yearb. Biol. Anthropol. 181, 58–80 (2023).
- Hunt, K. D. et al. Standardized descriptions of primate locomotor and postural modes. *Primates* 37, 363–387 (1996).
- Sugardjito, J. & van Hoof, J. A. R. A. M. Age-sex class differences in the positional behavior of the Sumatran orang-utan (*Pongo* pygmaeus abelii) in the Gunung Leuser National Park, Indonesia. Folia Primatol. 47, 14–25 (1986).
- Cant, J. G. H. Positional behavior of female Bornean orangutans (Pongo pygmaeus). Am. J. Primatol. 12, 71–90 (1987).
- Fleagle, J. G. Locomotion and posture of the Malayan siamang and implications for hominoid evolution. *Folia Primatol.* 26, 245–269 (1976).
- Hunt, K. D. Mechanical implications of chimpanzee positional behavior. Am. J. Phys. Anthropol. 86, 521–536 (1991).
- Hunt, K. D. Positional behavior in the Hominoidea. *Int. J. Primatol.* 12, 95–118 (1991).

- Hunt, K. D. Positional behavior of *Pan troglodytes* in the Mahale Mountains and Gombe Stream National Parks, Tanzania. *Am. J. Phys. Anthropol.* 87, 83–105 (1992).
- Doran, D. M. & McNeilage, A. Gorilla ecology and behavior. *Evol. Anthropol.* 6, 120–131 (1998).
- Doran, D. M. Sex differences in adult chimpanzee positional behavior: the influence of body size on locomotion and posture. *Am. J. Phys. Anthropol.* 91, 99–115 (1993).
- Doran, D. M. Comparative locomotor behavior of chimpanzees and bonobos: the influence of morphology on locomotion. *Am. J. Phys. Anthropol.* 91, 83–98 (1993).
- Gebo, D. L. Climbing, brachiation, and terrestrial quadrupedalism: historical precursors of hominid bipedalism. *Am. J. Phys. Anthropol.* 101, 55–92 (1996).
- Pontzer, H. & Wrangham, R. W. Climbing and the daily energy cost of locomotion in wild chimpanzees: implications for hominoid locomotor evolution. J. Hum. Evol. 46, 317–335 (2004).
- Tuttle, R. H. & Watts, D. P. The positional behavior and adaptive complexes of Pan gorilla. In Primate Morphophysiology, Locomotor Analyzes, and Human Bipedalism (ed. Kondo, S.) 261–288 (University of Tokyo Press, 1985).
- Mittermeier, R. A. Locomotion and posture in Ateles geoffroyi and Ateles paniscus. Folia Primatol. 30, 161–193 (1978).
- DeSilva, J. M. Vertical climbing adaptations in the anthropoid ankle and midfoot: Implications for locomotion in Miocene catarrhines and Plio-Pleistocene hominins. Ph.D. thesis, University of Michigan (2008).
- Cartmill, M. Pads and claws in arboreal locomotion. In *Primate Locomotion*(ed. Jenkins, F.) 45–83 (Academic Press, New York, 1974).
- Cartmill, M. Climbing. In *Functional Vertebrate Morphology* (ed. Hildebrand, M.) 73–88 (Harvard University Press, 1985).
- Jungers, W. L. The functional significance of skeletal allometry in Megaladapis in comparison to living prosimians. *Am. J. Phys. Anthropol.* 49, 303–314 (1978).
- Hirasaki, E., Kumakura, H. & Matano, S. Kinesiological characteristics of vertical climbing in *Ateles geoffroyi* and *Macaca fuscata*. Folia Primatol. 61, 148–156 (1993).
- DeSilva, J. M. Functional morphology of the ankle and the likelihood of climbing in early hominins. *Proc. Natl Acad. Sci. USA* 106, 6567–6572 (2009).
- Preuschoft, H. What does "arboreal locomotion" mean exactly and what are the relationships between "climbing", environment and morphology?. Z. Morph. Anthrop. 83, 171–188 (2002).
- Latimer, B., Ohman, J. C. & Lovejoy, C. O. Talocrural joint in African hominoids: implications for Australopithecus afarensis. Am. J. Phys. Anthropol. 74, 155–175 (1987).
- Holowka, N. B., O'Neill, M. C., Thompson, N. E. & Demes, B. Chimpanzee ankle and foot joint kinematics: arboreal versus terrestrial locomotion. *Am. J. Phys. Anthropol.* 164, 131–147 (2017).
- Püschel, T. A., Marcé-Nogué, J., Gladman, J. T., Bobe, R. & Sellers, W. L. Inferring locomotor behaviours in Miocene New World monkeys using finite element analysis, geometric morphometrics and machine-learning classification techniques applied to talar morphology. J. R. Soc. Interface 15, 20180520 (2018).
- Turley, K. & Frost, S. R. The shape and presentation of the catarrhine talus: a geometric morphometric analysis. *Anat. Rec.* 296, 877–890 (2013).
- Dunn, R. H., Tocheri, M. W., Orr, C. M. & Jungers, W. L. Ecological divergence and talar morphology in gorillas. *Am. J. Phys. Anthropol.* 153, 526–541 (2014).
- McNutt, E. J., Zipfel, B. & DeSilva, J. M. The evolution of the human foot. Evol. Anthropol. 27, 197–217 (2018).

- DeSilva, J., McNutt, E., Benoit, J. & Zipfel, B. One small step: a review of Plio-Pleistocene hominin foot evolution. *Am. J. Phys. Anthropol.* 168, 63–140 (2019).
- Harper, C. M., Roach, C. S., Goldstein, D. M. & Sylvester, A. D. Morphological variation of the *Pan* talus relative to that of *Gorilla. Am. J. Biol. Anthropol.* 181, 545–563 (2023).
- Friesen, S. E. et al. Shape variation in the talus and medial cuneiform of chimpanzees and bonobos. *Am. J. Biol. Anthropol.* 183, e24571 (2024).
- Monclús-Gonzalo, O. et al. A dryopithecine talus from Abocador de Can Mata (Vallès-Penedès Basin, NE Iberian Peninsula): morphometric affinities and evolutionary implications for hominoid locomotion. Am. J. Biol. Anthropol. 186, e70043 (2025).
- Gunnel, G. F. & Ciochon, R. L. Revisiting primate postcrania from the Pondaung Formation of Myanmar: the purported anthropoid astragalus. In *Elwyn Simons: A Search for Origins* (eds Fleagle, J. G. & Gilbert, C. C.) 211–228 (Springer, New York, 2008).
- Gebo, D. L. & Simons, E. L. Morphology and locomotor adaptations of the foot in early Oligocene anthropoids. *Am. J. Phys. Anthropol.* 74, 83–101 (1987).
- Harrison, T. New postcranial remains of Victoriapithecus from the middle Miocene of Kenya. J. Hum. Evol. 18, 3–54 (1989).
- Ward, C. V., Walker, A., Teaford, M. F. & Odhiambo, I. Partial skeleton of *Proconsul nyanzae* from Mfangano Island, Kenya. *Am. J. Phys. Anthropol.* 90, 77–111 (1993).
- Harrison, T. Small-bodied apes from the Miocene of East Africa. PhD thesis, University of London (1982).
- Langdon, J. H. Functional morphology of the Miocene hominoid foot. Contrib. Primatol. 22, 1–225 (1986).
- Nakatsukasa, M. et al. Hind limb of the Nacholapithecus kerioi holotype and implications for its positional behavior. Anthropol. Sci. 120, 235–250 (2012).
- Szalay, F. S. & Langdon, J. H. The foot of *Oreopithecus*: an evolutionary assessment. *J. Hum. Evol.* 15, 585–621 (1986).
- Marzke, M. W. et al. Comparative 3D quantitative analyses of trapeziometacarpal joint surface curvatures among living catarrhines and fossil hominins. Am. J. Phys. Anthropol. 141, 38–51 (2010).
- Gebo, D. L. & Schwartz, G. T. Foot bones from Omo: implications for hominid evolution. Am. J. Phys. Anthropol. 129, 499–511 (2006).
- 52. McInnes, D. G. Notes on the East African Miocene Primates. *J. East Afr. Uganda Nat. Hist. Soc. Nairobi* **17**, 141–181 (1943).
- 53. Birchette, M. The postcranial skeleton of *Paracolobus chemeroni*. PhD thesis, Harvard University (1982).
- Stirton, R. A. & Savage, D. E. A new monkey from the La Venta Miocene of Colombia. Compl. Est. Geol. Ofic. Colomb. 8, 345–356 (1951).
- Marivaux, L. et al. A platyrrhine talus from the early Miocene of Peru (Amazonian Madre de Dios sub-Andean Zone). J. Hum. Evol. 63, 696–703 (2012).
- Kay, R. F., Johnson, D. & Meldrum, D. J. A new pitheciin primate from the middle Miocene of Argentina. *Am. J. Primatol.* 45, 317–336 (1998).
- Gebo, D. L., Dagosto, M., Rosenberger, A. L. & Setoguchi, T. New platyrrhine tali from La Venta, Colombia. *J. Hum. Evol.* 19, 737–746 (1990).
- Meldrum, D. J. New fossil platyrrhine tali from the early Miocene of Argentina. Am. J. Phys. Anthropol. 83, 403–418 (1990).
- Nozaki, S., Oishi, M. & Ogihara, N. Talar trochlear morphology may not be a good skeletal indicator of locomotor behavior in humans and great apes. Sci. Rep. 11, 24063 (2021).
- Wunderlich, R. E. & Ischinger, S. B. Foot use during vertical climbing in chimpanzees (*Pan troglodytes*). J. Hum. Evol. 109, 1–10 (2017).
- Patel, B. A., Orr, C. M. & Jashashvili, T. Strength properties of extant hominoid hallucal and pollical metapodials. *J. Hum. Evol.* 143, 102774 (2020).

- Kozma, E. E. et al. Hip extensor mechanics and the evolution of walking and climbing capabilities in humans, apes, and fossil hominins. *Proc. Natl Acad. Sci. USA* 115, 4134–4139 (2018).
- Gebo, D. Plantigrady and foot adaptation in African apes: implications for hominid origins. *Am. J. Phys. Anthropol.* 89, 29–58 (1992).
- 64. Zeininger, A., Schmitt, D. & Wunderlich, R. E. Mechanics of heelstrike plantigrady in African apes. *J. Hum. Evol.* **145**, 102840 (2020).
- Prang, T. C. Rearfoot posture of *Australopithecus sediba* and the evolution of the hominin longitudinal arch. *Sci. Rep.* 5, 17677 (2015).
- Holowka, N. B. & O'Neill, M. C. Three-dimensional moment arms and architecture of chimpanzee (*Pan troglodytes*) leg musculature. *J. Anat.* 223, 610–628 (2013).
- 67. Keith, A. Man's posture: its evolution and disorders. *Br. Med. J.* **1**, 451–454, 499–502, 545–548, 587–590, 624–626, 669–672 (1923).
- Stern, J. T. Before bipedality. Yearb. Phys. Anthropol. 19, 59–68 (1975).
- Kimura, T., Okada, M. & Ishida, H. Kinesiological characteristics of primate walking. In *Environment, Behavior, and Morphology: Dynamic Interactions in Primates* (eds Morbeck, M. E., Preuschoft, H. & Gomberg, N.) 297–311 (G. Fischer, New York, 1979).
- Prost, J. H. Origin of bipedalism. *Am. J. Phys. Anthropol.* 52, 175–189 (1980).
- Fleagle, J. G. et al. Climbing: a biomechanical link with brachiation and with bipedalism. Symp. Zool. Soc. Lond. 48, 359–375 (1981).
- Cartmill, M. & Milton, K. The lorisiform wrist joint and the evolution of 'brachiating' adaptations in the Hominoidea. *Am. J. Phys. Anthropol.* 47, 249–272 (1977).
- Richmond, B. G., Begun, D. R. & Strait, D. S. The origin of human bipedalism: the knuckle-walking hypothesis revisited. *Yearb. Phys. Anthropol.* 44, 70–105 (2001).
- Alexander, R. M. Principles of Animal Locomotion (Princeton University Press, 2003).
- 75. Fleagle, J. G., Baden, A. L., Gilbert, C. C. *Primate Adaptation and Evolution* (Academic Press, 2024).
- Russo, G. A. et al. An ape partial postcranial skeleton (KNM-NP 64631) from the Middle Miocene of Napudet, northern Kenya. J. Hum. Evol. 192, 103519 (2024).
- Young, J. W., Russo, G. A., Fellmann, C. D., Thatikunta, M. A. & Chadwell, B. A. Tail function during arboreal quadrupedalism in squirrel monkeys (*Saimiri boliviensis*) and tamarins (*Saguinus Oedipus*). *JEZ-A* 323, 556–566 (2015).
- Grabowski, M., Hatala, K. G. & Jungers, W. L. Body mass estimates of the earliest possible hominins and implications for the last common ancestor. J. Hum. Evol. 122, 84–92 (2018).
- Williams, S. A. & Pilbeam, D. Homeotic change in segment identify derives the human vertebral formula from a chimpanzee-like one. *Am. J. Phys. Anthropol.* 176, 283–294 (2021).
- Richmond, B. G. & Strait, D. S. Evidence that humans evolved from a knuckle-walking ancestor. *Nature* 404, 382–385 (2000).
- 81. Tocheri, M. W., Orr, C. M., Jacofsky, M. C. & Marzke, M. W. The evolutionary history of the hominin hand since the last common ancestor of *Pan* and *Homo. J. Anat.* **212**, 544–562 (2008).
- 82. Pilbeam, D. R. & Lieberman, D. E. Reconstructing the last common ancestor of chimpanzees and humans. In *Chimpanzees and Human Evolution* (eds Muller, M. N., Wrangham, R. W. & Pilbeam, D. R.) 22–141 (Harvard University Press, 2017).
- 83. Almécija, S., Smaers, J. B. & Jungers, W. L. The evolution of human and ape hand proportions. *Nat. Commun.* **6**, 7717 (2015).
- Böhme, M. et al. A new Miocene ape and locomotion in the ancestor of great apes. *Nature* 575, 489–493 (2019).
- Drummond-Clarke, R. C. et al. Wild chimpanzee behavior suggests that a savanna-mosaic habitat did not support the emergence of hominin terrestrial bipedalism. Sci. Adv. 8, eadd9752 (2022).

- Williams, S. A., Prang, T. C., Meyer, M. R., Russo, G. A. & Shapiro, L.
 J. Reevaluating bipedalism in *Danuvius*. *Nature* 586, E1–E3 (2020).
- Boyer, D. M. & Seiffert, E. R. Patterns of astragalar fibular facet orientation in extant and fossil primates and their evolutionary significance. *Am. J. Phys. Anthropol.* **151**, 420–447 (2013).
- Ruff, C. B., Burgess, M. L., Squyres, N., Junno, J. A. & Trinkaus, E. Lower limb articular scaling and body mass estimation in Pliocene and Pleistocene hominins. J. Hum. Evol. 115, 85–111 (2018).
- Burgess, M. L., McFarlin, S. C., Mudakikwa, A., Cranfield, M. R. & Ruff, C. B. Body mass estimation in hominoids: age and locomotor effects. *J. Hum. Evol.* 115, 36–46 (2018).
- Perry, J. M., Cooke, S. B., Connour, J. A. R., Burgess, M. L. & Ruff, C. B. Articular scaling and body mass estimation in platyrrhines and catarrhines: modern variation and application to fossil anthropoids. *J. Hum. Evol.* 115, 20–35 (2018).
- Ishida, H., Kunimatsu, Y., Takano, T., Nakano, Y. & Nakatsukasa, M. Nacholapithecus skeleton from the Middle Miocene of Kenya. J. Hum. Evol. 46, 69–103 (2004).
- Grabowski, M., Hatala, K. G., Jungers, W. L. & Richmond, B. G. Body mass estimates of hominin fossils and the evolution of human body size. J. Hum. Evol. 85, 75–93 (2015).
- Patel, B. A., Yapuncich, G. S., Tran, C. & Nengo, I. O. Catarrhine hallucal metatarsals from the early Miocene site of Songhor, Kenya. *J. Hum. Evol.* 108, 176–198 (2017).
- 94. Grafen, A. The phylogenetic regression. *Philos. Trans. R. Soc. Lond. B Biol. Sci.* **326**, 119–157 (1989).
- 95. Pagel, M. Inferring the historical patterns of biological evolution. *Nature* **401**, 877–884 (1999).
- 96. Orme, D. et al. Package 'caper' (2023).
- R. Core Team. R: A Language And Environment For Statistical Computing (R foundation for Statistical Computing, Vienna, Austria, 2024).
- 98. Schneider, C. A., Rasband, W. S. & Eliceiri, K. W. NIH Image to ImageJ: 25 years of image analysis. *Nat. Methods* **9**, 671–675 (2012).
- Tocheri, M. W. et al. Functional capabilities of modern and fossil hominid hands: three-dimensional analysis of trapezia. *Am. J. Phys. Anthropol.* 122, 101–112 (2003).
- Tocheri, M. W., Razdan, A., Williams, R. C. & Marzke, M. W. A 3D quantitative comparison of trapezium and trapezoid relative articular and nonarticular surface areas in modern humans and great apes. *J. Hum. Evol.* 49, 570–586 (2005).
- Elliot, M. G. & Mooers, A. O. Inferring ancestral states without assuming neutrality or gradualism using a stable model of continuous character evolution. *BMC Evol. Biol.* 14, 1–15 (2014).
- Arnold, C., Matthews, L. J. & Nunn, C. L. The 10kTrees Website: a new online resource for primate phylogeny. *Evol. Anthropol.* 19, 114–118 (2010).
- Maddison, W. P. & Maddison, D. R. Mesquite: a modular system for evolutionary analysis. Version 3.81 http://www.mesquiteproject.org (2023).
- Simons, E. L. New faces of Aegyptopithecus from the Oligocene of Egypt. J. Hum. Evol. 16, 273–289 (1987).
- Kay, R. F. The phyletic relationships of extant and fossil Pitheciinae (Platyrrhini, Anthropoidea). J. Hum. Evol. 19, 175–208 (1990).
- Deino, A. L. & Hill, A. ⁴⁰Ar/³⁹Ar dating of Chemeron Formation strata encompassing the site of hominid KNM-BC 1, Tugen Hills, Kenya. *J. Hum. Evol.* 42, 141–151 (2002).
- 107. Seiffert, E. R., Simons, E. L. & Simons, C. V. M. Phylogenetic, biogeographic, and adaptive implications of new fossil evidence bearing on crown anthropoid origins and early stem catarrhine evolution. In *Anthropoid Origins: New Visions* (eds Ross, C. F. & Kay, R. F.) 157–181 (Springer, 2004).
- Kay, R. F. et al. The anatomy of *Dolichocebus gaimanensis*, a stem platyrrhine monkey from Argentina. *J. Hum. Evol.* 54, 323–382 (2008).

- 109. Kay, R. F. Biogeography in deep time—what do phylogenetics, geology, and paleoclimate tell us about early platyrrhine evolution?. Mol. Phylogenet. Evol. 82, 358–374 (2015).
- Bloch, J. I. et al. First North American fossil monkey and early Miocene tropical biotic interchange. *Nature* 533, 243–246 (2016).
- Harrison, T. New fossil anthropoids from the middle Miocene of East African and their bearing on the origin of the Oreopithecidae. Am. J. Phys. Anthropol. 71, 265–284 (1986).
- 112. Pugh, K. D. Phylogenetic analysis of Middle-Late Miocene apes. *J. Hum. Evol.* **165**, 103140 (2022).
- Revell, L. J. phytools: an R package for phylogenetic comparative biology (and other things). *Meth. Ecol. Evol.* 2, 217–223 (2012).
- Jungers, W. L., Falsetti, A. B. & Wall, C. E. Shape, relative size, and size-adjustments in morphometrics. *Am. J. Phys. Anthropol.* 38, 137–161 (1995).

Acknowledgements

Y. Assefa, D. Abebaw, the Ethiopian Authority for Research and Conservation of Cultural Heritage (ARCCH), T. White, G. Suwa, O. Lovejoy, and B. Asfaw facilitated access to the fossil talus of Ardipithecus ramidus used in this study. L. Berger, B. Zipfel, S. Jirah, and the fossil access committee of the Evolutionary Studies Institute at the University of the Witwatersrand facilitated access to the original South African fossil material. E. Westwig, A. Marcato, E. Hoeger (American Museum of Natural History), D. Lunde (United States National Museum of Natural History), L. Jellema and Y. Haile-Selassie (Cleveland Museum of Natural History), J. Chupasko and M. Omura (Harvard Museum of Comparative Zoology), T. White (Human Evolutionary Research Center at the University of California, Berkeley), H. Taboada (Center for the Study of Human Origins at New York University), C. Conroy (Museum of Vertebrate Zoology at Berkeley), W. Wendelen and E. Gilissen (Royal Museum for Central Africa), and the curatorial staff at the Field Museum of Natural History provided access to museum specimens. Doug Boyer provided access to 3D models of anthropoid tali originally appearing in Boyer and Seiffert (2013) and funded by NSF grant BCS 1317525. These files were downloaded from www.MorphoSource.org. Duke University. This work was supported by a Wenner-Gren Foundation Dissertation Fieldwork Grant (T.C.P.).

Author contributions

Conceptualization: T.C.P. and M.W.T. Methodology: T.C.P. and M.W.T. Investigation: T.C.P., M.W.T., B.A.P., S.A.W., and C.M.O. Visualization: T.C.P. Funding acquisition: T.C.P., M.W.T., B.A.P., S.A.W., and C.M.O. Writing—original draft: T.C.P. Writing—review and editing: M.W.T., B.A.P., S.A.W., and C.M.O.

Competing interests

The authors declare no competing interests.

Additional information

Supplementary information The online version contains supplementary material available at https://doi.org/10.1038/s42003-025-08711-7.

Correspondence and requests for materials should be addressed to Thomas C. Prang.

Peer review information *Communications Biology* thanks Zewdi J. Tsegai and the other anonymous reviewer(s) for their contribution to the peer review of this work. Primary Handling Editor: Johannes Stortz.

Reprints and permissions information is available at http://www.nature.com/reprints

Publisher's note Springer Nature remains neutral with regard to jurisdictional claims in published maps and institutional affiliations.

Open Access This article is licensed under a Creative Commons Attribution-NonCommercial-NoDerivatives 4.0 International License, which permits any non-commercial use, sharing, distribution and reproduction in any medium or format, as long as you give appropriate credit to the original author(s) and the source, provide a link to the Creative Commons licence, and indicate if you modified the licensed material. You do not have permission under this licence to share adapted material derived from this article or parts of it. The images or other third party material in this article are included in the article's Creative Commons licence, unless indicated otherwise in a credit line to the material. If material is not included in the article's Creative Commons licence and your intended use is not permitted by statutory regulation or exceeds the permitted use, you will need to obtain permission directly from the copyright holder. To view a copy of this licence, visit http://creativecommons.org/licenses/by-nc-nd/4.0/.

© The Author(s) 2025